Lab on a Chip

Label-free Enrichment of Human Adipose-Derived Stem Cells using a Continuous Microfluidic Sorting Cascade

Journal:	*Lab on a Chip*
Manuscript ID	LC-ART-12-2022-001138.R2
Article Type:	Paper
Date Submitted by the Author:	03-Mar-2023

Complete List of Authors:	Lee, Lap Man; CFD Research Corporation, Biomedical & Life Sciences Division Klarmann, George ; The Geneva Foundation Haithcock, Dustin; CFD Research Corporation, Biomedical & Life Sciences Division Wang, Yi; University of South Carolina, Mechanical Engineering Bhatt, Ketan; CFD Research Corporation, Biomedical & Life Sciences Division Prabhakarpandian, Balabhaskar ; CFD Research Corporation, Biomedical & Life Sciences Division Pant, Kapil ; CFD Research Corporation, Biomedical & Life Sciences Division Alvarez, Luis; Walter Reed National Military Medical Center Lai, Eva; University of Pittsburgh Swanson School of Engineering, Mechanical Engineering & Materials Science

SCHOLARONE™
Manuscripts

Label-free Enrichment of Human Adipose-Derived Stem Cells using a Continuous Microfluidic Sorting Cascade

Lap Man Lee[1], George J. Klarmann[2], Dustin W. Haithcock[1], Yi Wang[3], Ketan, H. Bhatt[1], Balabhaskar Prabhakarpandian[1], Kapil Pant[1], Luis M. Alvarez[4], and Eva Lai[5]

[1] CFD Research Corporation, 6820 Moquin Dr NW, Huntsville, AL, 35806, U.S.A.

[2] The Geneva Foundation, 9410 Key West Ave, Rockville, MD 20850, U.S.A.

[3] Mechanical Engineering, College of Engineering and Computing, University of South Carolina, 300 Main Street, Columbia, SC 29208, U.S.A.

[4] Walter Reed National Military Medical Center, 4494 Palmer Rd N, Bethesda, MD 20814, U.S.A.

[5] Mechanical Engineering & Materials Science, Swanson School of Engineering, University of Pittsburgh, 636 Benedum Hall, 3700 O'Hara Street, Pittsburgh, PA 15261, U.S.A

Abstract

Human adipose tissue is a rich source of mesenchymal stem cells (MSCs). Human adipose-derived stem cells (ADSCs) are first prepared by tissue digestion of lipoaspirate. The remaining constituent contains a mixture of ADSCs, other cell types and lysed fragments. We have developed a scalable microfluidic sorter cascade which enabled high-throughput and label-free enrichment of ADSCs prepared from tissue-digested human adipose samples to improve the quality of purified stem cell product. The continuous microfluidic sorter cascade was composed of spiral-shaped inertial and deterministic lateral displacement (DLD) sorters which separated cells based on size difference. The cell count characterization results showed >90% separation efficiency. We also demonstrated that the enriched ADSC sub-population by the microfluidic sorter cascade yielded 6× enhancement of expansion capacity in tissue culture. The incorporation of this microfluidic sorter cascade into ADSC preparation workflow facilitates the generation of transplantation-scale stem cell product. We anticipate our stem cell microfluidic sorter cascade will find a variety of research and clinical applications in tissue engineering and regeneration medicine.

1 Introduction

Human adipose tissue-derived stem cells (ADSCs) are self-renewable and multi-potent adult mesenchymal stem cells (MSCs), which can be differentiated into various cell types, including osteocytes, adipocytes, neural cells, vascular endothelial cells, cardiomyocytes, pancreatic β-cells, and hepatocytes, etc.[1] To date, approximately 130 clinical trials are being investigated to evaluate ADSC therapeutic efficacy and safety according to the US National Institutes of Health (NIH).[2] Therapeutic applications of ADSCs are broad, which include bone regeneration, fat reconstruction, cartilage and intervertebral disc regeneration, cardiovascular and myocardial regeneration, treatment of stroke and Parkinson's disease, hepatic regeneration, and pancreatic regeneration.[1] The increasing popularity of ADSCs is due to several reasons. First, the use of ADSCs raises fewer ethical concerns. In contrast to human embryonic stem cell (ESCs), which involves the destruction of a 5-day-old preimplantation embryo,[3] ADSCs are adult stem cells deriving from postnatal tissues. Second, ADSCs can be repeatedly harvested with lipoaspirate, which is routinely discarded as a by-product. With increasing obese population in the U.S., approximately 400,000 liposuction procedures are performed each year. Each extraction yields a large quantity (100 ml to >3 liters) of lipoaspirate.[4] Third, the average abundance of ADSCs in lipoaspirate-processed nucleated cells is approximately 2% compared with 0.002% bone marrow stem cell content in the total stromal cell population. The yield of ADSCs from 1g fat is approximately 5,000 cells, compared with 100 to 1,000 stem cells from 1mL bone marrow. The yield of ADSCs has been reported to exceed that from bone marrow by about 500-fold.[5–9] Fourth, ADSCs have good proliferative capacity and multipotency. ADSCs can be cultured for up to 1 month and retain strong multi-differentiation potential after 25 passages.[10,11] Fifth, clinical research on ADSCs has shown effective immunomodulation and reduced side effects of chronic immunosuppression in allotransplantation.[12,13] Last, the use of autologous additive platelet-rich plasma (PRP) in ADSCs has shown stimulatory effects in cell proliferation and differentiation for tissue regenerative therapies.[14–16] The efficacy of ADSCs and PRP had been confirmed in the healing process of chronic skin wounds,[17] neocartilage regeneration,[18] and osteoarthritis.[19] The synergistic effects of ADSCs and PRP were also studied in preclinical animal studies in the pressure injury model,[20] and the ischemic hindlimb model.[21]

ADSCs are first prepared by liposuction, collagenase digestion, and centrifugation to discard oil and tissue-lysed fragments. The remaining constituent is called stromal vascular fraction (SVF), which consists of a heterogeneous mixture of ADSCs, pericytes, monocytes/macrophages, endothelial, progenitor, and hematopoietic stem cells.[22] Amongst different cell types, ADSCs comprise 1–10% of the SVF cell population.[23] Typically, ADSCs are harvested by plastic adherence along with other cell types in the SVF

mixture. The ADSC sub-population adheres to plastic surfaces and expands in ADSC-specific growth media. The purity of ADSCs increases progressively in higher passages as other unattached cell types are washed out in the passaging process. It has been reported that the ADSC culture is almost completely purified upon three passages.[24] Commercially available immunoaffinity magnetic activated cell sorting (MACS) kits can be used to isolate ADSCs from human lipoaspirate with several hours of labor-intensive preparation steps. Currently, only one MACS cell separation kit, the CliniMACS® CD34 from Miltenyi Biotec was granted Food and Drug Administration (FDA) approval to isolate hematopoietic stem cells derived from donor blood after apheresis.[25]

Microfluidic sorting provides a minimally manipulated approach to enrich ADSC sub-population from tissue-digested SVF mixtures. With improved purity, ADSC co-culture samples are less susceptible to unpredictable influences from other SVF cell types.[26] The incorporation of microfluidic technology into existing ADSC preparation workflows also reduces the risk of contamination by allowing stem cell processing in an enclosed and Good Manufacturing Practices (GMP) environment for improved reproducibility, biosafety, and therapeutic efficacy.[27]

Two types of label-free microfluidic separation technologies have been developed to sort stem cells. Spiral inertial microfluidic sorting uses differential lift force to balance with Dean vortex-induced drag to separate bioparticles with different sizes.[28] Spiral inertial microfluidic sorters have higher throughput of several mL/min, but lower size separation resolution and low purity.[29] Spiral inertial microfluidic sorting devices have been developed to isolate differentiated neural stem cells (NSCs) from a mixture of induced pluripotent stem cells (iPSCs),[30] mouse MSCs from bone-marrow samples,[31] single cells from neurosphere clusters,[32] and sub-population of MSCs into osteoprogenitor with chondrogenic potential.[33,34] Deterministic lateral displacement (DLD) is another passive microfluidic sorting technology that uses steric effects to sort cells.[35] Different-sized cells are diverted into different flow paths when traversing through arrays of slanted micro-posts. DLD microfluidic sorters have lower throughput rates of several hundred μL/min but higher size resolution and high purity. A DLD microfluidic sorting device has been reported to separate particles with a resolution down to 10nm.[36] DLD technology has been recently applied to enrich primary human skeletal progenitor cells from bone marrow for bone regenerative therapies without the use of biomarkers.[37]

The sorting performance and functionality of these microfluidic sorters can be augmented when arranged in multi-step configuration and multi-module combination. Five subgroups of different-sized MSCs were sorted in the same spiral inertial microfluidic sorter in four rounds at different flow rates.[34] Three spiral inertial microfluidic sorters were cascaded on the same chip by balancing the fluidic resistance at the bifurcation.[38] Two separation branches were cascaded in the same integrated spiral microfluidic sorter to

enable two-step continuous cell sorting.[39] A microfluidic monolithic chip comprising modules of DLD, inertial focusing, and magnetophoresis was developed to continuously sort rare circulating tumor cells (CTCs) and deplete blood cells at high throughput.[40] A serial workflow comprised of label-free inertial microfluidic isolation and downstream leukocyte functional assessment by isodielectric separation has been developed for the severity evaluation of sepsis patients.[41] Recently, a novel two-stage i-DLD sorter coupling inertial microfluidics with DLD has been developed to separate spiked tumor cells from the diluted blood sample.[42]

In this work, combining the advantages of both spiral inertial and DLD sorters, we developed a label-free microfluidic sorter cascade to continuously enrich ADSCs from tissue-digested human lipoaspirate based on their size difference. The spiral inertial microfluidic sorter was optimized to recover ADSCs and reduce sample volume. The DLD microfluidic sorters were optimized to discard SVF and further improve sample purity. The sorting performance of this novel microfluidic sorter cascade was characterized using fluorescently labeled ADSCs spiked in the SVF cell mixture. Next, the enriched native ADSC sub-populations from the SVF cell sample by microfluidic sorting were tested for proliferation capacity.

2 Methods and materials

2.1 Microfluidic sorter cascade

The microfluidic sorter cascade consisted of one spiral inertial microfluidic sorter and two identical DLD microfluidic sorters (Figure 1). Inertial microfluidic sorting used the balance between differential lift force (inertial wall lift and velocity gradient force) and Dean vortex drag in a curvilinear fluidic channel to separate cells based on their size difference. The spiral microfluidic sorter was designed to focus larger ADSCs closed to the inner wall. Dominated by spanwise vortical re-circulation of Dean drag, other smaller SVF cell types and tissue-digested fragments tended to spread across the channel width. The enriched sample collected from the inner outlet of the inertial microfluidic sorter, which still contained a background of smaller debris was sent to two DLD microfluidic sorters for further purification.

DLD microfluidic sorting used arrays of slanted micro-posts to exert different magnitudes of steric force on cells for size-based separation.[35] Larger ADSCs had hydrodynamic centers of mass further away from

the micro-posts and were laterally displaced from the channel centerline to the side. Smaller SVF cells and fragments had the hydrodynamic center of mass closer to the micro-posts and traversed through the micro-post arrays in a zigzag manner along the channel centerline. As these two cell populations flowed downstream, the difference in lateral displacement was accumulated and directed to different outlets.

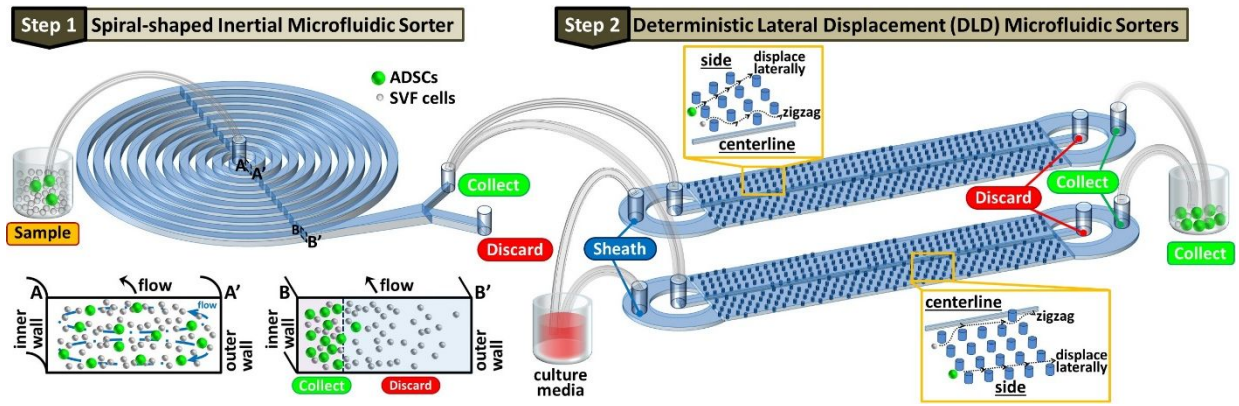

Figure 1. Schematic of continuous microfluidic enrichment for human adipose-derived stem cells (ADSCs) from tissue-digested stromal vascular fraction (SVF) cells using a serial combination of one spiral inertial and two identical deterministic lateral displacement (DLD) microfluidic sorters.

2.1.1 Design of the spiral inertial microfluidic sorter

The geometric design of the spiral inertial microfluidic stem cell sorter was adapted from our previous works.[29,31] The inertial microfluidic device consisted of a main 10-looped spiral microfluidic channel with a rectangular cross-section. The channel width was 500μm, and the total length was about 50cm connecting with one inlet and two outlets. The outlet channel split location was designed to optimize for ADSC recovery. The outlet portion near the inner side was designated for ADSC collection.

2.1.2 Design of the DLD microfluidic sorter

The DLD microfluidic sorter was designed to sort ADSCs from SVF cell samples. Each DLD microfluidic sorter contained two sets of symmetric slanted micro-post DLD arrays, which were separated by a centerline separator spanning the entire length of the device. Two symmetric sets of DLD arrays were connected to one common sheath inlet, sample inlet, collect outlet and discard outlet. The sorting characteristics of DLD was determined by the geometrical arrangement of the slanted angle and separation distance (both along

the streamwise and lateral directions) between each micro-post.[35] These parameters determined the cut-off (or critical) diameter. We chose the cut-off diameter based on size difference between ADSCs and other SVF cell types to maximize ADSC recovery and SVF cell discard. The size distribution of ADSCs and ADSC-depleted SVF cell sub-population will be characterized in Section 3.1. Larger ADSCs displaced laterally were collected by the side outlet channel. The SVF cells and fragments with the size smaller than the critical diameter traversed through the micro-post array in a "zigzag" path. They were not laterally displaced and collected by the discard outlet along the centerline. The detailed design parameters of the DLD microfluidic sorter were described in SI (Fig. S1, Table S1, and Fig. S2).

2.1.3 Device fabrication process

Both layouts of the spiral inertial and DLD microfluidic sorters were designed with AutoCAD (Autodesk, 2010LT). The photomasks were printed on a high-resolution transparency manufactured by CAD/Art Services, Inc. (Bandon, OR). Both spiral inertial and DLD microfluidic sorters were fabricated using polydimethylsiloxane (PDMS) soft-lithography technique. A single layer of SU-8 photoresist was patterned on 4" silicon wafers as mold masters. Photoresists SU-8 2075 and SU-8 3050 were used in the fabrication of spiral inertial and the the DLD microfluidic sorter mold masters respectively to accommodate for height difference of two devices. The SU-8 patterning processes were adapted from the manufacturer protocol from MicroChem data sheet (https://kayakuam.com/products/su-8-photoresists/). After SU-8 patterned silicon mold master fabrication, the average height of the SU-8 patterned layers of the spiral inertial and the DLD microfluidic sorter device measured 155μm and 40μm, respectively, using a profilometer. PDMS was prepared by mixing base with curing agent at weight ratio of 1:10 (Sylgard 184, Dow Corning) and cast over the SU-8 patterned silicon masters, followed by degassing in a desiccator and curing in an oven at 65°C for at least 3 hours. The cured PDMS substrates were peeled off from the SU-8 patterned silicon masters and diced, followed by inlet/outlets hole punching (1.5mm diameter). For device assembly, the PDMS substrates and glass microscope slides were treated in an air plasma cleaner (Harrick Plasma, Ithaca, NY), and then bonded together permanently. Different parts of a fabricated DLD microfluidic sorter device were shown under phase imaging of optical microscopy in SI (Fig. S3).

2.2 Sample Preparation

2.2.1 Reagents and media

Human MesenCult™ MSC basal medium, Human MesenCult™ MSC stimulatory supplement, L-Glutamine (L-Glut), Dulbecco's phosphate-buffered saline (D-PBS) without calcium and magnesium, and trypsin-EDTA (0.25%) from STEMCELL Technologies, Inc. (Vancouver, Canada) were primarily used for tissue culture of ADSCs. CellTracker™ Red and Green dyes, Gibco™ Minimum Essential Media (MEM), NucBlue® fixed cell ReadyProbes® reagent (DAPI), and Pierce™ 16% formaldehyde were purchased from ThermoFisher Scientific Inc. Bovine Serum Albumin (BSA) was purchased from Fisher Scientific (Hampton, NH). All other chemicals were purchased from Sigma-Aldrich (St. Louis, MO).

2.2.2 Preparation of SVF cells from tissue digestion of lipoaspirate

Isolation of SVF cell population from human lipoaspirate was prepared using a protocol adapted from a previous publication.[43] Human lipoaspirate was purchased from Zen-Bio, Inc. (Research Triangle Park, NC). Lipoaspirate was first washed with equal volumes of phosphate buffer saline (PBS) and Penicillin-Streptomycin (Pen/Strep), optionally with anti-fungal amphotericin B, mixed and settled over several minutes. The bottom phase was aspirated off. This process was repeated until liquid was clear in order to remove most of the red and white blood cells. The tissue was re-suspended in equal volume of sterile filtered PBS containing 0.1% collagenase Type I from Worthington Biochemical (Lakewood, NJ) and 0.5% BSA which was pre-warmed to 37°C. The suspension was incubated at 37°C for 30–60 min with agitation every 5–10 minutes until the fat was transformed into a smooth looking paste lacking obvious fat chunks. The sample was centrifuged at 300×g for 5 min at the room temperature. After centrifugation, the whole sample was shaken vigorously to remix and disrupt ADSCs from adipocytes and re-spun as before. The material was aspirated above the pellet while being careful not to disturb the SVF pellet. The pellet was re-suspended in alpha-MEM/10% Fetal Bovine Serum (FBS), L-Glut/Pen/strep in 10mL. The re-suspended SVF cell mixture was passed through a 70μm cell strainer in a 50ml conical centrifuge tube to remove any connective tissue, and the sample was centrifuged at 300×g for 5 min. The media was aspirated and cells were re-suspended at 3×10^6 cells/mL of freezing media (80%FBS/10% alpha-MEM/10% Dimethyl sulfoxide (DMSO)). The SVF vials were then cryopreserved in liquid nitrogen.

2.2.3 Preparation of human adipose-derived stem cell (ADSC) culture

The ADSC sub-population from SVF cell mixture was purified by plastic adherence in tissue culture at 37°C and 5% CO_2. The SVF cell mixture containing native ADSCs was plated at 2.3×10^6 cells per T75 flask. The media was refreshed twice a week. The ADSC culture was washed with D-PBS to remove residual blood cells before one week incubation. Tissue culture-purified ADSCs were sub-cultured to higher passages or cryopreserved in a similar protocol with the SVF preparation. To reconstitute purified and cryopreserved ADSCs, after thawing the cryopreserved ADSC vial in a warm water bath at 37°C, culture media was added to the ADSC samples. The ADSC suspension was collected by centrifugation at 300×g for 10 min to remove DMSO in the freezing media and then re-suspended in culture media. The purified ADSCs (5×10^5 cells) were seeded in tissue culture flask. Typically, after 3–4 days, the ADSC culture achieved 80–90% confluency and was sub-cultured at a splitting ratio of 1:3.

2.2.4 Reconstitution of ADSCs and ADSCs-depleted SVF cell samples

Passages P3 to P6 of cultured ADSCs were used in all microfluidic sorting experiments and characterization assays. ADSC tissue culture at 80–90% confluency was dissociated with 0.25% trypsin-EDTA for 10min, centrifuged to remove the trypsin at 300×g for 10min, and re-suspended in cell culture media at desired concentration and volume. The SVF cell population contained 1–10% of native ADSCs.[23] To correctly characterize sorting performance using fluorescently labeled ADSC spiking samples, it was necessary to remove the native ADSC sub-population in the SVF cell samples before microfluidic sorting experiments. Native ADSCs in SVF samples expressed cell membrane receptors which bind with plastic surface and plastic adherence has been used to purifiy ADSCs.[24] To prepare ADSC-depleted SVF cell sub-population, cryopreserved SVF samples from lipoaspirate were first thawed in a water bath at 37°C and reconstituted carefully in ADSC culture media. The SVF cell suspension was then centrifuged at 300×g for 10min. After discarding the supernatant which contained freezing media, the SVF pellets were re-suspended in ADSC culture media. The SVF cells were incubated in a T75 culture flask (37°C, 5% CO_2) for about 4 hours. Native ADSCs in the SVF adhered to the culture flask, which were validated by immunophentotyping using immunocytochemistry staining from our previous work.[29] The cell suspension was then collected as a sub-population of SVF cells depleted of native ADSCs. The cell suspension was filtered with a 40μm cell strainer to screen out large clumps.

2.2.5 CellTracker™ fluorescent staining protocol

Adherent ADSCs in tissue culture flasks were washed with PBS and stained with 5μM CellTracker™ Green in serum-free culture media for 20min. The stained ADSCs were washed thoroughly with PBS with centrifugation to remove unbound dye. The ADSCs were then dissociated in culture media, centrifuged and reconstituted at desired concentration and volume in ADSC culture media. The cell concentration was confirmed with hemocytometer cell counting. We had attempted to stain the ADSC-depleted SVF cell sub-population with CellTracker™ Red. However, we found that the ADSC-depleted SVF sub-population contained a considerable amount of cell fragments and debris which did not uptake the fluorescent dye. We used phase imaging to count ADSC-depleted SVF cells and fragments.

2.3 Sorting Performance Characterization

2.3.1 Cell counting

Purified ADSCs loaded with CellTracker™ fluorescent dye were used to spike the tissue-digested SVF mixture to enable cell count for sorting performance characterization of our microfluidic sorter cascade. The ADSCs were counted under fluorescent imaging and the issue-digested SVF cells without fluorescent labeling were counted under brightfield phase imaging. Cell samples were counted with 10μL aliquots using a hemocytometer mounted on an epifluorescence microscope (Nikon TiE) under a 10× objective with phase imaging. Fluorescence or brightfield images were taken at 6×6 fields of view and exported to ImageJ (https://imagej.nih.gov/ij/) for image analysis and cell count. Typically, more than a total number of thousand cells and tens of targeted ADSCs were counted.

2.3.2 Sorting performance metrics CellTracker™ stained samples

We defined the sorting performance characterization metrics as follows:

$$Purity = \frac{[\text{ADSC}]}{[\text{ADSC}] + [\text{SVF cell}]} \quad (1)$$

$$Recovery[\text{ADSC}]_{Collect} = \frac{[\text{ADSC}]_{Collect}}{[\text{ADSC}]_{Collect} + [\text{ADSC}]_{Discard}} \quad (2\text{–a})$$

$$Recovery[\text{SVF cell}]_{Collect} = \frac{[\text{SVF cell}]_{Collect}}{[\text{SVF cell}]_{Collect} + [\text{SVF cell}]_{Discard}} \quad (2\text{–b})$$

$$Recovery[\text{ADSC}]_{Discard} = \frac{[\text{ADSC}]_{Discard}}{[\text{ADSC}]_{Collect} + [\text{ADSC}]_{Discard}} \quad (2\text{–c})$$

$$Recovery[\text{SVF cell}]_{Discard} = \frac{[\text{SVF cell}]_{Discard}}{[\text{SVF cell}]_{Collect} + [\text{SVF cell}]_{Discard}} \quad (2\text{–d})$$

$$Enrichment\ Ratio = \frac{Purity_{Collect}}{Purity_{Inlet}} \quad (3)$$

where [ADSC] and [SVF cell] denoted the number of ADSCs and SVF cells respectively.

2.3.3 Proliferation assay

The purity and quality of a stem cell population can be evaluated by its expansion capability in proliferation assays.[24] The cell cultures were incubated at 37°C and 5% CO_2 with media changes twice a week. At each passage, once the tissue culture reached 80–90% confluency, the cells were trypsinized with 0.25% trypsin-EDTA for 10 minutes. After washing out the Trypsin-EDTA with centrifugation, the cell pellets were re-suspended in fresh media and cell counted with a hemocytometer before plating back to a larger well plate or culture flask to best match optimized seeding densities ($2.5–10\times10^3$ cells per cm^2). We continued the tissue culture of ADSCs to higher passages until they lost their expansion capability such that they failed to double their population for two weeks. The cell proliferation was calculated using the following equation:[44]

$$N = N_0 e^{kt} \quad (4)$$

where N_0 is the number of cells in the beginning, k is the growth rate, and t is the time. The doubling time, T is calculated as:

$$T = \frac{ln2}{k} \quad (5)$$

2.3.4 Continuous Microfluidic Sorter Cascade

The microfluidic sorter cascade consisted of one spiral inertial sorter, one Y-splitter, and two identical DLD sorters assembled in a 3-D printed plastic casing (Figure 2a). Inertial microfluidic sorters typically operate at higher flow rates than the DLD microfluidic sorters. We matched the flow rate between the two types of sorters by connecting the collect outlet of the spiral inertial microfluidic sorter to the sample inlets of two DLD microfluidic sorters through a Y-splitter device using 0.020" inner diameter Tygon™ tubing. The Y-splitter was a symmetric bifurcation device. The widths of the parent and daughter channels were 400μm and 200μm, respectively. Both parent and daughter channels were 5mm long. The height of all channels was 100μm. The flow rates were matched between these two types of microfluidic sorters to enable continuous sorting. The connection of two DLD microfluidic sorters and Y-splitter dramatically increased the fluidic resistance of the collect outlet of the spiral inertial microfluidic sorter. To prevent backflow and balance the fluidic resistance between the collect and discard outlets in the spiral inertial microfluidic sorter, a Tygon™ tubing with a length of 20cm and an inner diameter of 0.010" was inserted to the discard outlet of the spiral inertial microfluidic sorter. The length of this flow restrictive tubing was experimentally determined to match fluidic resistance between the Y-splitter and two DLD microfluidic sorters. The discard outlets of the inertial microfluidic sorters and the two DLD microfluidic sorters were directed to a common reservoir in a 12-well plate. Two collect outlets of the two DLD microfluidic sorters were directed to another common reservoir in the 12-well plate. Prior to use, all microfluidic devices in the assembly were primed in one single step to remove any trapped air bubbles. Alternatively, isopropanol (IPA) could be used in the priming process for sterilization treatment. When the cell samples arrived the sorting region of both inertial and DLD sorters, the flow conditions had reached steady state for optimal sorting performance. We determined this experimental setup and operational flow rates by several optimization steps as reported in SI (Fig. S4 to Fig. S8).

The optimal inlet sample flow rates were set in the inertial microfluidic sorter to be 500μL/min and the sheath flows of each DLD microfluidic sorter to be 200μL/min. The cell sample mixture mounted on a single syringe pump (Harvard Apparatus) was connected to the sample inlet of the spiral inertial

microfluidic sorter. Two syringes filled with culture media mounted on a dual syringe pump (Harvard Apparatus) were connected to the sheath flow inlet of each DLD microfluidic sorter. The detailed workflow and flow rates at each device unit and connection component in the microfluidic sorter cascade assembly are shown in Figure 2b.

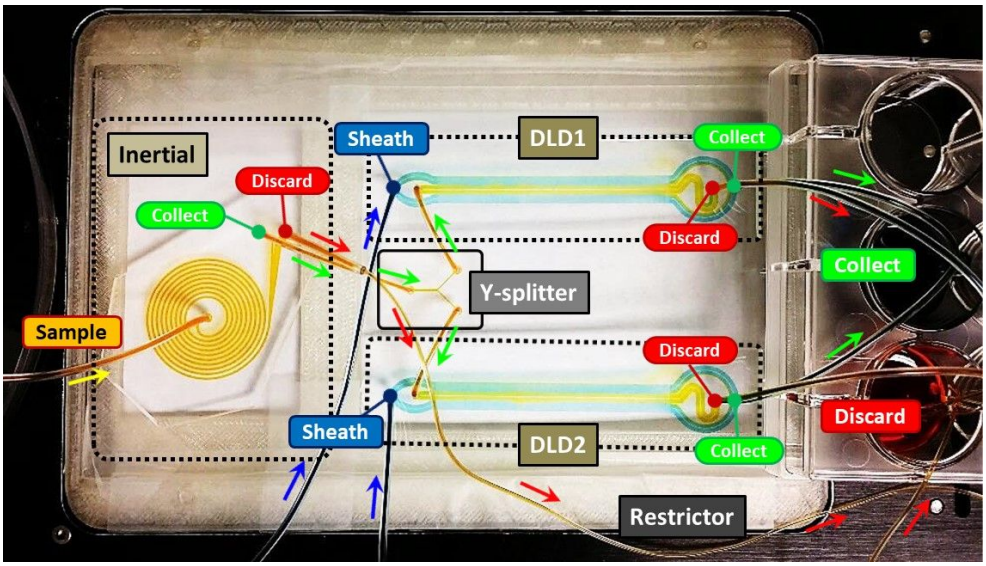

(a)

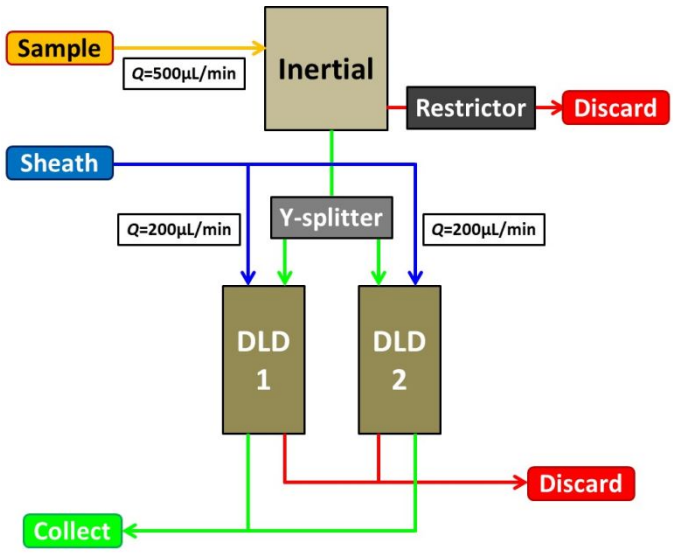

(b)

Figure 2. Microfluidic sorter cascade for ADSC sorting: (a) experimental assembly; and (b) schematic.

3 Results and Discussion

3.1 Size Distribution of ADSC and ADSC-depleted SVF Cell Sub-population

We examined the size distribution of ADSC, SVF cell, and ADSC-depleted SVF cell sub-populations. Cell samples were loaded into a hemocytometer and inspected manually under an optical microscope with phase imaging. The diameter of purified ADSCs was 20.6±4.3μm (mean±s.d., n=373), SVF cells 16.9±5.4μm (n=372), and ADSC-depleted SVF cells 12.0±2.4μm (n=373). The average cell diameter of ADSC-depleted SVF cells was about 60% of the purified ADSCs. Two sub-populations were statistically different based on Student's t test. Our findings agreed reasonably well with published data.[45] The size distribution of these cell sub-populations was shown in SI (Fig. S9).

3.2 Sorting Performance Characterization with Fluorescent Labeled ADSCs

We characterized the sorting performance of the microfluidic sorter cascade using CellTracker™ Green stained ADSCs spiked in ADSC-depleted SVF cell mixture. The preparation of the ADSC-depleted SVF cell mixture and fluorescent labeling protocol were described in Section 2.2.4 and Section 2.2.5 respectively. The cell sample mixture was prepared (~1×10^6 cells/mL) with initial purity between 1–2%. The integrated microfluidic sorter cascade ran continuously for 6min with inlet sample processing volume about 3mL. Approximately 3×10^6 cells were processed. Cell samples from the inlet, collect, and discard outlets were imaged and counted as shown in Figure 3a. The cells that showed green color in fluorescent imaging were labeled ADSCs. The non-stained cells and tissue-digested fragments were from the SVF sub-population, which were counted under phase imaging. The average sorting performance was summarized in Figure 3b, Figure 3c, and Table 1. The continuous-flow, sequential microfluidic enrichment approach resulted in targeted ADSC enrichment of □30×, from an initial purity of 1.7% to 46.8%, ADSC recovery of >90%, and non-target SVF cell discard of >95%. A sample sorting throughput of □8,000 cells/s was achieved.

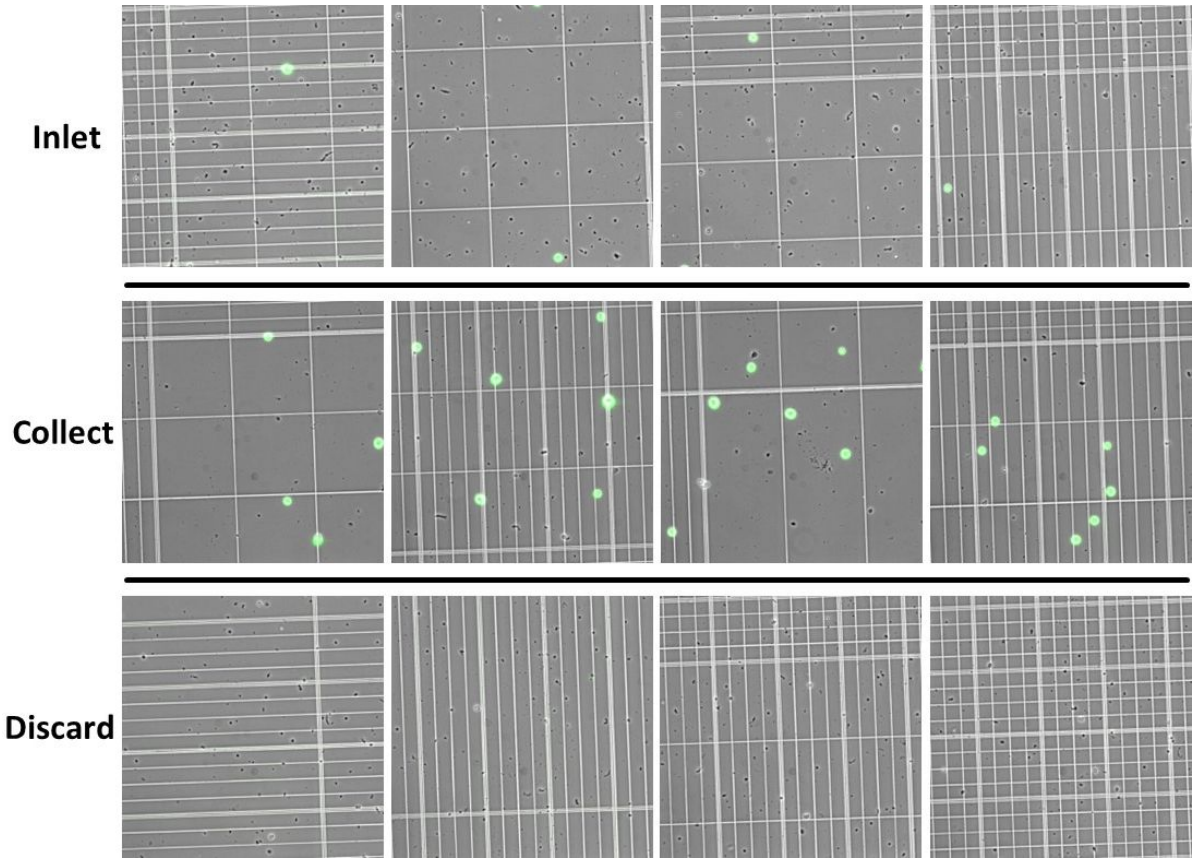

(a)

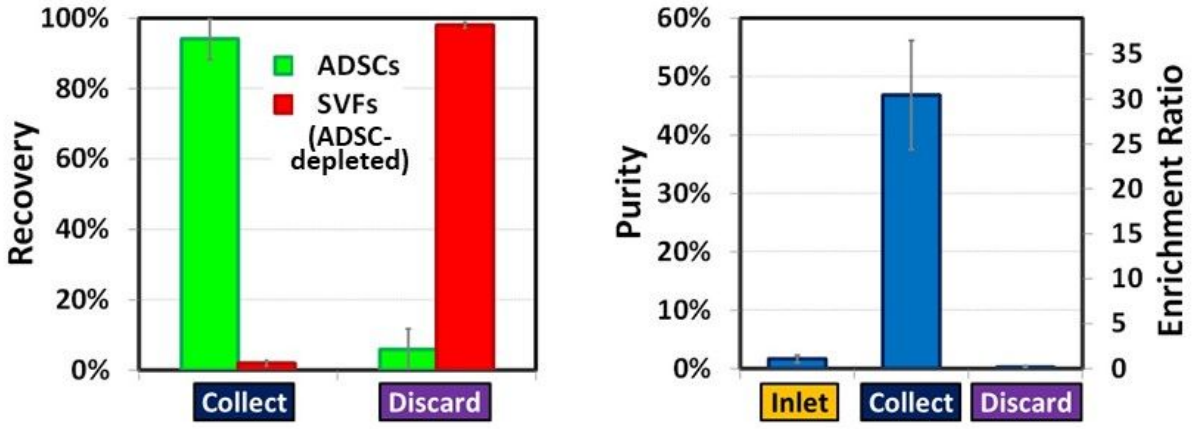

(b) *(c)*

Figure 3. Sorting performance of ADSCs (green) from ADSCs-depleted SVF cell mixture by microfluidic sorter cascade: (a) cells collected at inlet and outlets in a hemocytometer under fluorescence imaging and phase microscopy; (b) recovery; and (c) enrichment ratio and purity.

Table 1. Sorting performance of ADSCs from ADSCs-depleted SVF cell mixture by microfluidic sorter cascade.

Purity			Recovery				Enrichment
Inlet	Collect	Discard	Collect		Discard		Collect
			ADSCs	SVF cells	ADSCs	SVF cells	
1.7%	46.8%	0.2%	94.1%	1.9%	5.9%	98.1%	30.4×

SVF cells were ADCS-depleted

3.3 Expansion Capacity of ADSC Sub-population after Microfluidic Enrichment

A proliferation assay was used to quantify the expansion capability of native ADSC sub-population from the SVF cell mixture in tissue culture after microfluidic sorting. Cryopreserved SVF cell vials were thawed in culture media and passed through a 40μm pore-size cell strainer to screen out large clumps. After washing out the freezing media with centrifugation, the native SVF cells were re-suspended in fresh media at 1×10^6 cells/mL. 5 mL of this native SVF cell mixture preparation was used directly as the inlet sample. The microfluidic sorter cascade was run for 10 minutes at the prescribed operating condition. After microfluidic sorting, cell concentrations from the collect and discard outlets were 7×10^4 cells/mL and 1×10^6 cells/mL, respectively. Cell samples at the inlet without microfluidic sorting and those from the collect and discard outlets after microfluidic sorting were transferred into a 24-well plate with equivalent seeding density of 3×10^5 cells per well.

We conducted proliferation assays on cell samples of inlet, collect, and discard, as described in Section 2.3.2. The number of harvested cells at each passage for three samples was counted using a hemocytometer as shown in Figure 4a. We determined ADSC expansion doubling time by logarithmic fitting based on equation (4) – (5) in Figure 4b. Overall, the microfluidics-enriched native ADSC sub-population in the SVF mixture, known as the collect sample, was expanded □300× over one month of tissue culture in 6 passages. In addition, about 4,000 cells, around 1.3% of the SVF cell population attached to the 24-well plate initially were able to proliferate afterwards, compared with only about 1,500 cells, less than 0.5% in the case of SVF samples without microfluidic enrichment, which is the original sample supplied at the inlet. Our calculation found that the doubling time of the microfluidics-enriched ADSC sub-population was $T = 4.2$ days or 101 hours. When we evaluated the proliferation rate at P3-P6 of microfluidics-enriched ADSCs, the expansion doubling time was $T = 3.0$ days or 72 hours, which is comparable with the doubling time of completely purified ADSCs (P3-P9) at $T = 86 \pm 23$ hours from published data.[24,46] In comparison with SVF cell samples without microfluidic enrichment, the number of harvested ADSCs with microfluidic sorting was expanded only □50× after one month of culture. The expansion doubling time of ADSCs in the SVF sample without

microfluidic sorting was T = 5.6 days or 134 hours. The doubling time of ADSC–SVF samples from discard outlet with microfluidic sorting was T = 9.2 days or 221 hours. The cell expansion doubling time of all samples was summarized in Table 2. The tissue culture images at each passage were shown in SI (Fig. S10). The reduced proliferation doubling time confirmed that our microfluidic sorter cascade successfully enriched the ADCS cell content from tissue-digested sample.

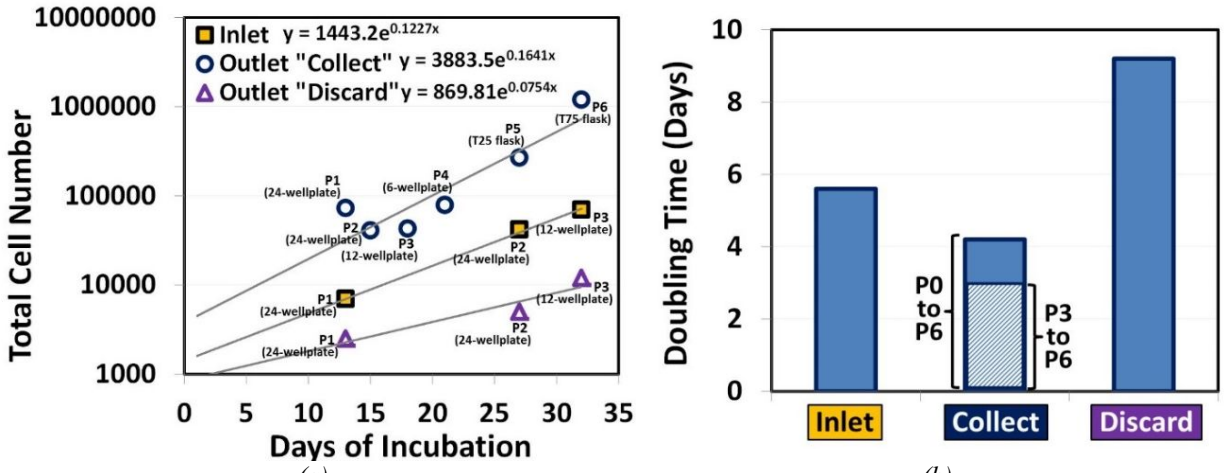

(a) (b)

Figure 4. Expansion of ADSC sub-population enriched from SVF cell mixture after microfluidic sorting: (a) number of ADSCs harvested at different passages; and (b) population doubling time.

Table 2. Comparison of expansion doubling time of ADSC sub-population enriched from SVF samples after microfluidic sorting.

	Inlet	Collect		Discard
		P0-P6	P3-P6	
in days	5.6	4.2	3.0	9.2
in hours	134	101	72	221

Conclusion

In this work, we developed a novel microfluidic sorter cascade for label-free, continuous and rapid isolation of human ADSCs from tissue-digested lipoaspirate products. This microfluidic sorter cascade combines the advantages of both spiral inertial and DLD microfluidic sorters to isolate targeted ADSCs from other SVF

cell types and fragments based on size difference. No additional biochemical labeling steps were required for device operation. PDMS soft-lithography techniques was used to fabricate individual microfluidic sorter devices and components, which were readily assembled in a 3-D printed casing.

Spiral inertial microfluidic sorters can separate cells with higher throughput but with lower size resolution, while the DLD microfluidic cell sorters have higher size resolution but operate at lower throughput.. Thus, both sorters are combined in the microfluidic sorter cascade for their complementary characteristics. We first used a spiral inertial microfluidic sorter to recover most ADSCs, discard the majority of other SVF cell types and tissue digested fragments, and reduce processing volume. After spiral inertial microfluidic sorting, the sample solution was split and supplied to two identical DLD microfluidic sorters to further enrich ADSCs from SVF cell mixtures.

Using CellTracker™ stained spiking ADSC samples, we demonstrated that this cascade microfluidic enrichment approach achieved targeted ADSC enrichment of □30× and recovery of >90%, non-target SVF cells discard of >95%, and sorting throughput rate of 8,000 cells/s, resulting in 200× improvement in comparison with dielectrophoresis (DEP) microfluidic sorters.[47,48] Despite the high enrichment ratio, the final purity of ADSCs in SVF cells was about 50%. The impurities collected after DLD microfluidic sorting consisted of cell aggregates and other larger non-target cells, which have similar size with target ADSCs and are challenging to separate out using size-based sorting methods alone. We also demonstrated that microfluidic sorting improved the quality of ADSC tissue culture by removal of contaminant SVF cell types. In a proliferation assay, we demonstrated the microfluidic enriched ADSC sub-population from SVF mixture improved by 6× in expansion capacity in 6 passages of one-month tissue culture.

Label-free and transplantation-capacity scale microfluidic sorting technology will open up new avenues of intraoperative usages of stem cells, which avoids exposing stem cells to potentially harmful xenobiotic reagents and minimizes cell manipulation which could cause infectious contaminations. We anticiplate that our label-free, rapid, and minimally intrusive microfluidic sorting technology augments to streamline the stem cell preparation workflow in clinics and research labs for regenerative medicine and tissue engineering applications.

Author contributions

Lap Man Lee: formal analysis, investigation, visualization and writing – original draft; George J. Klarmann: sample acquisition, preparation and experimental characterization of SVFs, writing – review & editing; Dustin W. Haithcock: device fabrication; Yi Wang: conceptualization, funding acquisition, methodology development and writing – review & editing; Ketan, H. Bhatt: conceptualization, device design and writing – review & editing; Balabhaskar Prabhakarpandian: conceptualization, methodology and writing – review & editing; Kapil Pant: supervision and writing – review & editing; Luis M. Alvarez: supervision and writing – review & editing; Eva Lai: writing – review & editing.

Conflicts of interest

The authors report no conflicts of interest.

Acknowledgements

This research was sponsored by the U.S. Army Medical Research and Materiel Command (USAMRMC) under SBIR contract No. W81XWH-15-C-0112. Opinions, interpretations, conclusions and recommendations are those of the authors and are not necessarily endorsed by the U.S. Army.

Reference

1 L. Frese, P. E. Dijkman and S. P. Hoerstrup, *Transfus Med Hemother*, 2016, **43**, 268–274.

2 https://clinicaltrials.gov

3 N. M. P. King and J. Perrin, *Stem Cell Res Ther*, 2014, **5**, 85.

4 J. M. Gimble, A. J. Katz and B. A. Bunnell, *Circ Res*, 2007, **100**, 1249–1260.

5 S. Mohamed-Ahmed, I. Fristad, S. A. Lie, S. Suliman, K. Mustafa, H. Vindenes and S. B. Idris, *Stem Cell Res Ther*, 2018, **9**, 168.

6 Y.-C. Lin, H.-J. Harn, P.-C. Lin, M.-H. Chuang, C.-H. Chen, S.-Z. Lin and T.-W. Chiou, *Cell Transplant*, 2017, **26**, 449–460.

7 W. Tsuji, J. P. Rubin and K. G. Marra, *World J Stem Cells*, 2014, **6**, 312–321.

8 L. Mazini, L. Rochette, M. Amine and G. Malka, *Int J Mol Sci.*, 2019, **20**, 2523.

9 J. K. Frasern, I. Wulur, Z. Alfonso and M. H. Hedrick, *Trends Biotechnol*, 2006, **24**, 150–154.

10 K. L. Burrow, J. A. Hoyland and S. M. Richardson, *Stem Cells International*, 2017, **2017**, 2541275.

11 Y. Zhu, T. Liu, K. Song, X. Fan, X. Ma and Z. Cui, *Cell Biochem Funct*, 2008, **26**, 664–675.

12 R. Heyes, A. Iarocci, Y. Tchoukalova and D. G. Lott, *Journal of Transplantation*, 2016, **2016**, 6951693.

13 M. Waldner, W. Zhang, I. B. James, K. Allbright, E. Havis, J. M. Bliley, A. Almadori, R. Schweizer, J. A. Plock, K. M. Washington, V. S. Gorantla, M. G. Solari, K. G. Marra and J. P. Rubin, *Front Immunol.*, 2018, **9**, 1642.

14 R. P. Gersch, J. Glahn, M. G. Tecce, A. J. Wilson and I. Percec, *Aesthetic Surgery Journal*, 2017, **37**, 723–729.

15 T. Stessuk, M. B. Puzzi, E. A. Chaim, P. C. M. Alves, E. V. de Paula, A. Forte, J. M. Izumizawa, C. C. Oliveira, F. Frei and J. T. Ribeiro-Paes, *Arch Dermatol Res.*, 2016, **308**, 511–520.

16 P. Gentile, A. Orlandi, M. G. Scioli, C. Di Pasquali, I. Bocchini and V. Cervelli, *Stem Cells Transl Med.*, 2012, **1**, 230–236.

17 M. Conese, L. Annacontini, A. Carbone, E. Beccia, L. R. Cecchino, D. Parisi, S. Di Gioia, F. Lembo, A. Angiolillo, F. Mastrangelo, L. Lo Muzio and A. Portincasa, *Stem Cells International*, 2020, **2020**, 7056261.

18 J. Shen, Q. Gao, Y. Zhang and Y. He, *Mol Med Rep.*, 2015, **11**,1298–303.

19 J. Pak, J. H. Lee, K. S. Park, B. C. Jeong and S. H. Lee, *Biores Open Access*, 2016, **5**, 192–200.

20 Z. Liu, S. Xiao, K. Tao, H. Li, W. Jin, Z. Wei, D. Wang and C. Deng, *Stem Cells International*, 2019, **2019**, 3091619.

21 C. F. Chen and H. T. Liao, *World J Stem Cells*, 2018, **10**, 212–227.

22 L. Shukla, W. A. Morrison and R. Shayan, *Frontiers in Surgery*, 2015, **2**, 1–12.

23 M. O. Kilinc, A. Santidrian, I. Minev, R. Toth, D. Draganov, D. Nguyen, E. Lander, M. Berman, B. Minev and A. A. Szalay, *Clin Transl Med.*, 2018, **7**, 5.

24 H.-T. Chen, M.-J. Lee, C.-H. Chen, S.-C. Chuang, L.-F. Chang, M.-L. Ho, S.-H. Hung, Y.-C. Fu, Y.-H. Wang, H.-I Wang, G.-J. Wang, L. Kang and J.-K. Chang, *J Cell Mol Med*, 2012, **16**, 582–593.

25 B. D. Plouffe, S. K. Murthy and L. H. Lewis, *Rep Prog Phys*, 2015, **78**, 016601.

26 S. Blaber, R. Webster, C. J. Hill, E. J. Breen, D. ,Kuah, G. Vesey and B. R. Herbert, *J Transl Med*, 2012 **10**, 172.

27 L. Sensebé, M. Gadelorge and S. Fleury-Cappellesso, *Stem Cell Research & Therapy*, 2013, **4**, 66.

28 N. Herrmann, P. Neubauer and M. Birkholz, *Biomicrofluidics*, 2019, **13**, 061501.

29 L. M. Lee, Y. Wang, C. J. Garson, G. J. Klarmann, B. Prabhakarpandian, K. Pant, L. M. Alvarez and E. Lai, *The 21st International Conference on Miniaturized Systems for Chemistry and Life Sciences (MicroTAS 2017)*, 2017, Paper No. M188h.

30 H. Song, J. M. Rosano, Y. Wang, C. J. Garson, B. Prabhakarpandian, K. Pant, G. J. Klarmann, L. M. Alvarez and E. Lai, *Microfluidics and Nanofluidics*, 2017, **21**, 64.

31 L. M. Lee, J. M. Rosano, Y. Wang, G. J. Klarmann, C. J. Garson, B. Prabhakarpandian, K. Pant, L. M. Alvarez and E. Lai, *Anal. Methods*, 2018, **10**, 713–721.

32 S. S. P. Nathamgari, B. Dong, F. Zhou, W. Kang, J. P. Giraldo-Vela, T. L. Mcguire, R. McNaughton, C. Sun, J. Kessler and H. Espinosa, *Lab Chip*, 2015, **15**, 4591–4597.

33 W. C. Lee, H. Shi, Z. Poon, L. Nyan, T. Kaushik, G. Shivashankar, J. Chan, C. Lim, J. Han and K. V. Van Vliet, *Proc Natl Acad Sci U S A*, 2014, **111**, E4409–E4418.

34 L. Yin, Y. Wu, Z. Yang, C. A. Tee, V. Denslin, Z. Lai, C. Lim, E. Lee and J. Han, *Lab Chip*, 2018, **18**, 878–889.

35 J. McGrath, M. Jimenez and H. Bridle, *Lab Chip*, 2014, **14**, 4139–4158.

36 L. R. Huang, E. Cox, R. Austin and J. Sturm, *Science*, 2004, **304**, 987–990.

37 M. Xavier, S. H. Holm, J. Beech, D. Spencer, J. Tegenfeldt, R. Oreffo and H. Morgan, *Lab Chip*, 2019, **19**, 513–523.

38 M. Robinson, H. Marks, T. Hinsdale, K. Maitland and G. Coté, *Biomicrofluidics*, 2017, **11**, 024109.

39 T. H. Kim, H. J. Yoon, P. Stella and S. Nagrath, *Biomicrofluidics*, 2014, **8**, 064117.

40 F. Fachin, P. Spuhler, J. M. Martel-Foley, J. Edd, T. Barber, J. R. Walsh, M. Karabacak, V. Pai, M. Yu, K. C. Smith, H. Hwang, J. Yang, S. Shah, R. Yarmush, L. Sequist, S. Stott, S. Maheswaran, D. Haber, R. Kapur and M. Toner, *Scientific Reports*, 2017, **7**, 10936.

41 B. Jundi, H. Ryu, D.-H. Lee, R. Abdulnour, B. D. Engstrom, M. G. Duvall, A. Higuera, M. Pinilla-Vera, M. E. Benson, J. Lee, N. Krishnamoorthy, R. Baron, J. Han, J. Voldman and B. Levy, *Nature Biomedical Engineering*, 2019, **3**, 961–973.

42 N. Xiang, J. Wang, Q. Li, Y. Han, D. Huang and Z. Ni, *Anal. Chem.*, 2019, **91**, 10328–10334.

43 J. Li, J. Curley, Z. Floyd, X. Wu, Y. Halvorsen and J. Gimble, *Methods Mol Biol*, 2011, **702**, 17–27.

44 J. L. Sherley, P. B. Stadler and J. S. Stadler, *Cell Prolif.*, 1995, **28**, 137–144.

45 P. Bora and A. S. Majumdar, *Stem Cell Res Ther*, 2017, **8**, 145.

46 D. A. De Ugarte, K. Morizono, A. Elbarbary, Z. Alfonso, P. Zuk, M. Zhu, J. Dragoo, P. Ashjian, B. Thomas, P. Benhaim, I. Chen, J. Fraser and M. Hedrick, *Cells Tissues Organs*, 2003, **174**, 101–109.

47 M. Simon, Y. Li, J. Arulmoli, . P. McDonnell, A. Akil, J. Nourse, A. Lee and L. Flanagan, *Biomicrofluidics*, 2014, **8**, 064106.

48 H. Song, J. M. Rosano, Y. Wang, C. J. Garson, B. Prabhakarpandian, K. Pant, G. J. Klarmann, A. Perantoni, L. M. Alvarez and E. Lai, *Lab Chip*, 2015, **15**, 1320–1328.